 doi:10.20944/preprints201710.0156.v1

Article

Plant Fluorescence Measured under Two Extreme Lighting Conditions Using a Passive Spectroradiometer

Trina Merrick [1,*], Ralf Bennartz [1,2], Maria Luisa S. P. Jorge [1], Thiago S. F. Silva [3], John Rausch [1] and Guilherme Gualda [1]

[1] Department of Earth and Environmental Science, Vanderbilt University, 5726 Stevenson Center; 7th floor, Nashville, TN, U.S.A., 37240
[2] Space Science and Engineering Center, University of Wisconsin – Madison, 1225 W. Dayton St., Madison, WI, U.S.A., 53706
[3] Universidade Estadual Paulista (UNESP), Instituto de Geociências e Ciências Exatas, Campus de Rio Claro, Ecosystem Dynamics Observatory. Av. 24A, 1515, Bela Vista, 13506-900, Rio Claro, Brazil
* Correspondence: trina.l.merrick@vanderbilt.edu; Tel.: +xx-615-322-2976

Abstract: In this study, we evaluated chlorophyll fluorescence (CF) under two extreme illumination conditions at plant scale with a passive spectroradiometer. Fluorescence (*F*) was estimated by reading directly from radiance spectra of a variety of plants illuminated with light-emitting diode (LED) grow lights in the laboratory. Solar-induced fluorescence (SIF) was estimated from spectral measurements of the same plants under sunlight using the Fraunhofer Line Depth (FLD) method. Chlorophyll fluorescence yield (F_{yield}) and solar-induced fluorescence yield (SIF_{yield}) were calculated by normalizing *F* and SIF with absorbed photosynthetically active radiation (APAR). Two approaches to estimating APAR were compared: utilizing white reference spectra and reflected spectra versus white reference spectra combined with the fraction of absorbed photosynthetically active radiation (fPAR) derived from literature. Average F and SIF were different by a factor of approximately twenty-four ($F = 0.110 \pm 0.038$ $Wm^{-2}\mu m^{-1}sr^{-1}$ versus $SIF = 2.60 \pm 1.87$ $Wm^{-2}\mu m^{-1}sr^{-1}$). In contrast, the average normalized values F_{yield} and SIF_{yield} were within the margin of error of one another ($F_{yield} = 0.022 \pm 0.008$ $\mu m^{-1}sr^{-1}$ and $SIF_{yield} = 0.030 \pm 0.020$ $\mu m^{-1}sr^{-1}$). This study highlights the influence of APAR on CF and the importance of properly accounting for it when estimating yield and demonstrates the ability of two simple and portable experimental setups with a passive instrument to obtain fluorescence metrics.

Keywords: photosynthesis; carbon uptake; primary production; light use efficiency; measurement techniques; Oxygen bands; handheld spectrometer; Analytical Spectral Devices

1. Introduction

Understanding of plant health, vegetation functioning, and details of carbon uptake processes could be improved through innovative methods of monitoring photosynthesis from leaf to global scales. Chlorophyll fluorescence (CF) is an especially promising parameter to remotely sense photosynthetic status of plants. CF varies with changes in photochemistry and it is sensitive to environmental conditions, which make it especially suitable for measuring physiological traits and a better predictor of plant health and seasonality than broadband indices, such as the normalized difference vegetation index (NDVI) [1-4]. CF and heat from non-photochemical quenching are the two processes by which plants regulate excess energy input to the photosynthesis machinery. If combined with information about input illumination, these quantities reveal details about photosynthesis and have the potential to quantitatively determine parameters linked to physiological status of plants, carbon uptake, growth rates, and plant reactions to stress. Specifically, CF is the light energy emitted by a plant in the wavelength range of approximately 0.680-0.780 μm,

which generates an emission spectrum with two broad peaks. The first peak occurs around 0.680 μm and corresponds to activity from Photosystem II (PSII), while the second peak is at approximately 0.74 μm and corresponds to Photosystem I (PSI) activity. When measured under sunlight, the fluorescence signal is overpowered by the intensity of the reflected solar irradiance, with CF making up only from 1-5% of the reflected signal from vegetation. However, two atmospheric oxygen absorption windows intersect with the CF emission spectrum: the Oxygen-A (O_2A) band is within the PSI range at approximately 0.761μm and the Oxygen-B (O_2B) band is at approximately 0.687μm in close proximity to the PSII peak. Measurements centred at these bands enable comparisons between CF retrievals under sunlight and the full spectrum CF measured in the laboratory, provided the techniques properly account for insolation variability effects [5].

To distinguish between outdoor and laboratory CF measurements, we can refer to the measurements as solar-induced chlorophyll fluorescence (*SIF*) when CF is induced by sunlight, and fluorescence (*F*) when induced by any other source. Since *F* and *SIF* contain a combination of information about the photosynthetic status of vegetation and incident irradiance and are linked to photosynthesis, light use efficiency, and Gross Primary Production (GPP), measurements of this parameter and associated quantities are desirable both in the laboratory and field [6-12]. At the leaf scale, pulse-amplitude modulation (PAM) fluorimetry is one of the most commonly used methods of exploring the light reactions of photosynthesis due to its ability to monitor and manipulate the activity, status and efficiency of photosystem II (PSII) [1, 12]. The efficiency of PSII is a measure of the relative quantum yield and a proxy for light use efficiency. PAM, considered to be an active sensing technique, utilizes a modulated light source to trigger *F* and measures relative states of *F* accurately at the leaf scale. However, PAM is not well suited for experiments where radiometrically calibrated radiances are desired or for upscaling to plant level or beyond. Further, because PAM is bound by the limits of relative measurements, comparisons between studies, such as remote sensing studies, are difficult to accomplish [7, 9, 12-14]. *SIF*, measured through passive measurement techniques, has been demonstrated to be related to plant photosynthetic functioning and has been shown to be proportional to carbon uptake and gross primary production (GPP) [3, 15-18]. Studies also suggest *SIF* is an earlier indicator of vegetation stress than other remote sensing vegetative health indices [11, 19].

Despite *SIF*'s advantages, to our knowledge, there have been no published studies attempting to passively measure F in the laboratory with common LED grow lights or relate this type of measurement to retrievals of *SIF* from passive observations. Passive spectrometers collect measurements with the potential to determine *F*, *SIF*, and other fluorescence metrics. Additionally, spectroradiometers that operate only in the vis-NIR tend to be smaller, more portable, and less expensive, but just as good as the extended range systems for F and *SIF* measurements, so more studies should evaluate these instruments for fluorescence estimates. In this study, the instrument used was an ASD Handheld 2 Pro spectroradiometer (Analytical Spectral Devices/Panalytical, Boulder, CO.). ASD Field spectrometers specifically have been used in various studies for FLD retrievals estimating *SIF* [3, 18, 20-23]. The ASD Handheld 2 Pro spectroradiometer (HH2), which is used in this study, is small, has a fixed fiber optic, and can be operated untethered from a laptop. The HH2 has identical spectral and radiometric specifications to the ASD Field spectrometer in the 325-1075nm range, but is more portable and durable than the field spectrometer (**Figure 1**). While passive spectral measurements do not contain as much detailed information regarding the specific photochemistry as PAM measurements, they have the ability to estimate fluorescence in radiance units rather than relative units because of the HH2's absolute radiometric calibration. This allows for wider comparisons across experiments and the potential for more direct comparisons of plant functioning across different physiologies. Passive spectroscopy also has a greater capacity for scaling from leaf to plant, canopy, ecosystem or global scale [9, 12, 18].

The purpose of this study was to employ a relatively simple and inexpensive instrument and experimental setup to measure fluorescence quantities in radiance units with sufficient accuracy to account for the influence of the absorbed photosynthetically active radiation (APAR) on the values of *F* and *SIF*. We show these methods reliably estimate fluorescence metrics that under vastly

Preprints (www.preprints.org) | NOT PEER-REVIEWED | Posted: 24 October 2017 doi:10.20944/preprints201710.0156.v1

different insolation conditions. In order to accomplish this, *F* and *SIF* have to be estimated from the full spectral observations from the instrument. In addition, techniques to estimate APAR need to be established and evaluated. The heavily influential incident irradiance can be accounted for by normalizing *SIF* by the absorbed photosynthetically active radiation (APAR). The remaining quantity, termed fluorescence quantum yield [24], or SIF_{yield}, has been related to photosynthetic efficiency [11, 23] and has been shown to be a proxy for light use efficiency as a model parameter to estimate gross primary productivity [6]. As mentioned before, the yield of *F*, F_{yield}, is also related to light use efficiency.

In this study, we explored the potential of using observations from an ASD Handheld Pro 2 Spectroradiometer (HH2) (Analytical Spectral Devices/Panalytical, Boulder, CO) to estimate fluorescence (*F*) and Fluorescence yield (F_{yield}) of plants illuminated by a common light emitting diode (LED) in the laboratory and to estimate solar-induced fluorescence (*SIF*) and solar-induced fluorescence yield (SIF_{yield}), then compare these fluorescence metrics. The techniques presented are useful for future studies of relationships among F, *SIF*, and GPP quantities in both laboratory and field settings, as well as expanding scientific disciplines where passive remote sensing is used to determine the state of plant health at leaf, plant, and canopy scales.

The remainder of this article is structured as follows: In Section 2 we describe the experimental methods and calculations. Section 3 outlines the results of the experiments and a discussion and conclusions are given in sections 4 and 5, respectively. Since notation across the literature varies, a table of nomenclature was developed for this article found in Table A 1.

2. Materials and Methods

2.1. Spectral data collection

An ASD Handheld 2 Pro spectroradiometer was used to make all spectral observations. There were two experimental setups for the HH2: laboratory dark tent under light emitting diode (LED) illumination and outdoors under full sunlight. **Figure 1** shows the HH2 with a Spectralon® white reference panel in the dark tent with regular full spectrum lighting (a), with LED (b), with sunlight in a typical outdoor measurement (c) and in the case with accessories (d).

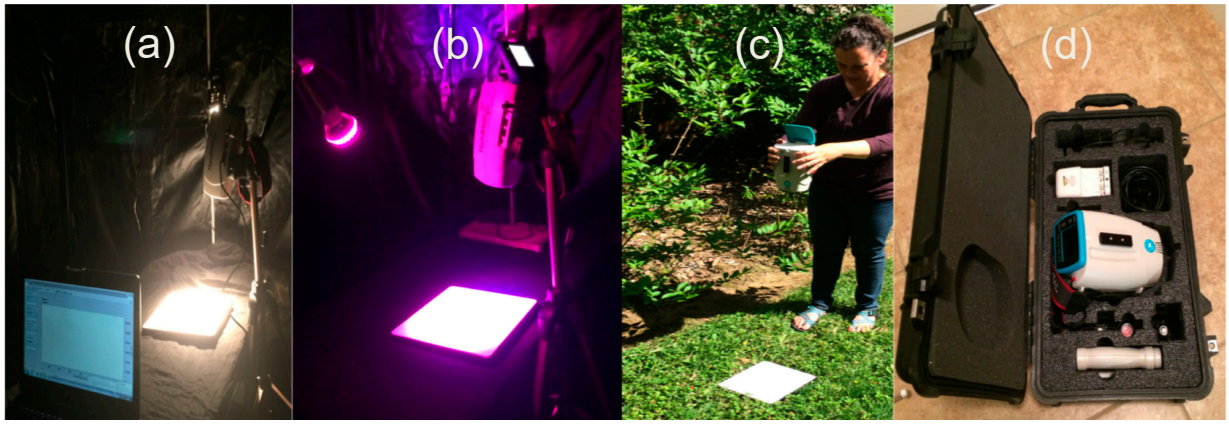

Figure 1. ASD Handheld 2 Pro Spectroradiometer a) set up in laboratory tethered mode with laptop and ASD Illuminator b) set up in laboratory untethered with light emitting diode MiracleLED™ c) in the field untethered and d) stored in Pelican™ case with all accessories.

For the experiments, a selection of both potted plants and plants growing outdoors (natural plants) were used. Table A 2 summarizes these plants and their characteristics. **Figure 2** shows a sample of the plants under LED along the top row with the matching plant under sunlight along the bottom row. For each plant target, a measurement was made with the HH2 in both illumination conditions (LED and sunlight) within 15 minutes of one another. In the laboratory under the LED, potted plants or cuttings of natural plants were placed in a 5′ x 6′ military surplus field dental x-ray development tent (dark tent) and their spectra recorded. The potted plants varied in size, structure,

Preprints (www.preprints.org) | NOT PEER-REVIEWED | Posted: 24 October 2017 doi:10.20944/preprints201710.0156.v1

type, and were all cared for according to instructions at purchase to maintain plant health. The natural plants chosen were visibly healthy with accessible portions for measurement. Spectra were recorded in both illumination conditions with the HH2 directly over the plants at a vertical distance insuring the field of view for the bare fiber optic did not extend past the margins of greenery and assuring inclusion of multiple leaves, needles, or branches. The vertical distance from the top of the plants was approximately 20 cm.

Figure 2. Sample of plants used in the experiment. Plants on the top row are under LED illumination. Bottom row are in sunlight. Plants L to R: Magnolia cuttings/natural, Pine cuttings/natural, Potted Variegated Lilyturf, Potted Pothos.

For all observations, the HH2 bare fiber optic (25° field of view) was used for acquisition. The instrument was set to average 25 individual measurements for each recorded spectrum. A white reference measurement was taken at a maximum of ten-minute intervals to capture environmental changes. Before each white reference measurement, the integration time was optimized automatically, which yields the maximum signal-to-noise ratio. The white reference panel measurements were taken from a distance of approximately 20 cm to match the distance from the plants as closely as possible. MiracleLED™ 2.2 Watt and a 7 Watt TOMTOP™ E27 LED grow lights were used in the laboratory. Grow LEDs emit a limited spectrum, primarily in red and blue regions, making fluorescence detectable in the 0.68-0.78 μm range. They were placed at a slight angle to the reference panel/plant target at a vertical distance of approximately 25 cm and oriented to illuminate the target as fully as possible.

2.2. Fluorescence estimates

The values for *F* under LED illumination were taken directly from the measured spectrum at the wavelength corresponding to the trough of the Oxygen-A (O_2A) absorption band, 0.761 μm, from laboratory observations. The Oxygen-B (O_2B) band trough is at 0.687 μm and a corresponding *F* value could be chosen for comparison to *SIF* values at that band. However, the O_2B has been shown to be less reliable when utilizing one of the FieldSpec (FS) spectroradiometers (Analytical Spectral Devices, Boulder, CO) [18, 20, 21]. The FS and HH2 have identical spectral resolution of 3 nm full width-half max and identical sampling interval of 1 nm [18, 25, 26]. This prompted close examination of the O_2B band, which corresponds to the PSII peak of the full spectrum. Due to the results presented in Section 3.1, the values for F at 0.687 μm were not used in the analyses.

Preprints (www.preprints.org) | NOT PEER-REVIEWED | Posted: 24 October 2017 doi:10.20944/preprints201710.0156.v1

2.3. Solar-induced fluorescence estimates

Spectra of the same potted plants or the naturally growing sources of cuttings measured indoors were recorded outdoors on the same date. Outdoor measurements were made first and every effort was made to transfer indoors as quickly as possible within 8-15 minutes of the outdoor measurements. Radiance based methods for retrieval of *SIF* are almost entirely derived from the Fraunhofer Line Depth (FLD) method [18], first proposed by Plascyk and Gabriel [27]. This method compares the radiance of a plant target spectrum to a reference panel placed under identical illumination conditions. By exploiting the FLD or "in-filling" of the Fraunhofer or Oxygen absorption bands, an estimate of *SIF* can be reached. Values from the measured spectra in this study were used to estimate *SIF* via the FLD method using the O_2A and O_2B bands. A measurement of the radiance inside and outside an oxygen absorption band of the target plant, L_{on} and L_{off}, respectively, is compared to an irradiance measurement inside and outside the same band for the reference, E_{on} and E_{off}.

To estimate L_{SIF} from these values, the system of equations

$$\begin{aligned} L_{on} &= RE_{on} + SIF_{on} \\ L_{off} &= RE_{off} + SIF_{off} \end{aligned} \quad (1)$$

are used. R_{on} and R_{off} are the reflectance coefficients in and out of the absorption band, which is the ratio between the energy flux reflected by a sample to the energy flux reflected by the reference panel for the same solid angle [27-29], but, for the FLD method, R_{on} is equal to R_{off}, thus R is used in Equation 1. SIF_{on} and SIF_{off} are the fluorescence in and out of the absorption band. For the standard FLD method, the R and *SIF* are assumed to be constant on the band and off the bands. Using this assumption, substituting and rearranging the above yields an equation for fluorescence:

$$SIF = \frac{E_{off}L_{on} - E_{on}L_{off}}{E_{off} - E_{on}} \quad (2)$$

The FLD method and its derivatives require selection of the wavelengths used for λ_{on} and λ_{off} within each oxygen absorption band, O_2A and O_2B of a spectrum. In other studies that employed the FLD method, the O_2B λ_{on} band is 0.687 or 0.688 μm and the O_2A λ_{on} band 0.760 or 0.761 μm [18]. The λ_{off} for each absorption region can have an even larger range depending on the instrument and experiment. Here, we examined the spectra of incoming sunlight measured with the HH2 from the white reference panel to assure the bands chosen for λ_{on} were in the lowest portion of the absorption band troughs and λ_{off} was clearly on the shoulder of the absorption band. In addition, the shape and depth of the absorption bands were examined to determine which absorption band would give the best results.

2.4. Fluorescence yield and solar-induced fluorescence yield calculations

In order to compare values of fluorescence between the two experimental setups, the difference in input radiation to the photosynthetic system between the sun and LEDs need to be addressed [19, 30]. This type of normalized fluorescence, termed fluorescence quantum yield, or fluorescence yield for short, (SIF_{yield}) [24], has been related to photosynthetic efficiency [23] and has been shown to be a suitable proxy for light use efficiency (LUE) as a model parameter to estimate GPP [6]. To calculate F_{yield} or SIF_{yield}, an estimate of the absorbed photosynthetically active radiation (APAR) is required for each observation [30-32]. In this study, two approaches to estimating APAR were taken and the results compared.

The illumination available to plants in the range of wavelengths useful for plant photosynthesis (approximately 400-700 nm), termed photosynthetically active radiation (PAR), is outlined in the literature [31-36]. The irradiance supplied by the LED or sunlight in the PAR range is available from the white reference spectrum recorded in conjunction with each plant spectrum measured and is used in each of the two methods for estimating APAR.

Preprints (www.preprints.org) | NOT PEER-REVIEWED | Posted: 24 October 2017 doi:10.20944/preprints201710.0156.v1

In our first approach, we estimated the degree to which the available energy, or PAR, is utilized by the plant by weighting PAR with the fraction of absorbed photosynthetically active radiation (fPAR) estimated at each wavelength by interpolating action spectrum data from Table V and Table III, respectively, in McCree [34] as outlined in Equation (3). The action spectrum of McCree [34] is reproduced in **Figure 3**.

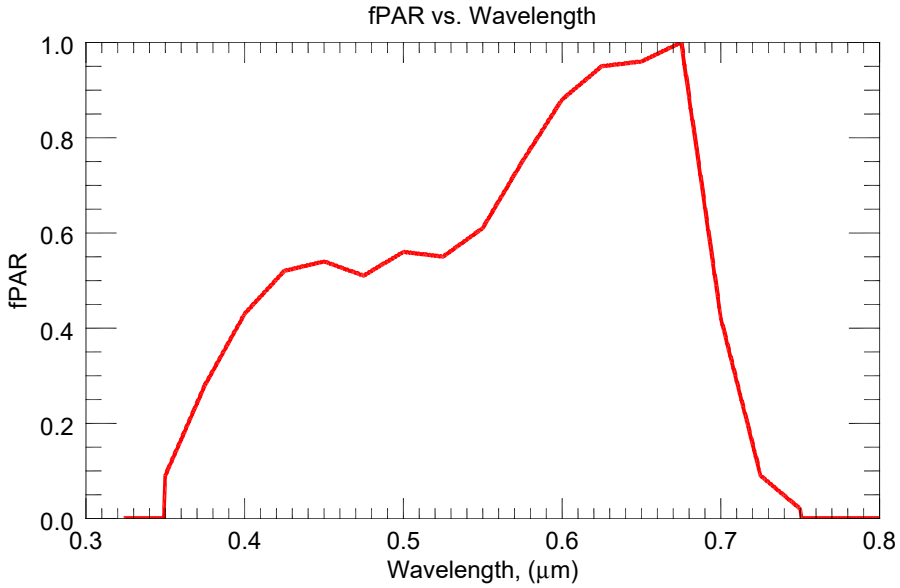

Figure 3. The fraction of photosynthetically active radiation values at each wavelength plotted as an "Action Spectrum"[34]. The values are interpolated from data over the range of PAR, 0.344-0.757μm. These data, this particular interpretation of the PAR range and the name "Action Spectrum" are derived from McCree [34] and Inada [33].

If the incoming irradiance, $E_i(\lambda)$ from 0.344 to 0.757 μm [33] in units of $Wm^{-2}\mu m^{-1}$ is considered the input to the photosynthetic machinery, or PAR, and fPAR is the fraction of absorbed photosynthetically active radiation from **Figure 3** [33, 34], then the Absorbed Photosynthetic Active Radiation using this technique ($APAR_\alpha$) is

$$APAR_\alpha = \int E_i(\lambda) fPAR(\lambda) d\lambda \quad (3)$$

in Wm^{-2} .

In the second approach, the difference in incoming and reflected spectra was tested as the basis for APAR, which we term $APAR_\delta$. If the coverage of the plant canopy is sufficiently thick to not allow exposure of the soil in the background, we can assume APAR can be estimated in $Wm^{-2}\mu m^{-1}$ based on the difference in incident and reflected plant target radiance in the Photosynthetically Active Radiation (PAR) range of 0.400 to 0.700μm as

$$APAR_\delta = \int_{0.400}^{0.700} \left[E_i(\lambda) - \pi L_{PAR}(\lambda) \right] d\lambda \quad (4)$$

where $E_i(\lambda)$ is the incident irradiance and $L_{PAR}(\lambda)$ is the reflected radiance. This approach is based on Damm, Elbers [6] and Li and Moreau [37]. This allows us to calculate normalized fluorescence, F_{yield}, as

$$F_{yield} = \frac{\pi F}{APAR} \quad (5)$$

Preprints (www.preprints.org) | NOT PEER-REVIEWED | Posted: 24 October 2017 doi:10.20944/preprints201710.0156.v1

and calculate normalized solar-induced chlorophyll fluorescence, SIF_{yield}, [38-40] using

$$SIF_{yield} = \frac{\pi SIF}{APAR} \quad (6)$$

having units of $\mu m^{-1} sr^{-1}$. Equations (5) and (6) can be applied either to $APAR_{\alpha}$ or $APAR_{\delta}$, so that the impact of different calculations of APAR can be compared.

2.5. Uncertainty estimates

The chlorophyll fluorescence (CF) signal is small compared to the overall reflected spectra from plants, whether it is observed in the lab or under sunlight. Here we discuss briefly, how uncertainty estimates for *SIF* and *F* are calculated.

The manufacturer supplied the signal-to-noise ratio (SNR) for the HH2 unit used in this study (Unit#1944). These SNR data were supplied by the manufacturer as a spectrum of SNR values for each wavelength. The average of the manufacturer's SNR spectrum for the HH2 is 6659.1, which corresponds to a relative error of 0.02% for measurements. As the SNR for an instrument varies by the power of the light source, and the CF signal from plants is small and dependent on incoming irradiance, and since our focus is on two extreme lighting conditions, the specific SNR for the HH2-LED experimental setup (SNR_{LED}) and the HH2-sunlight experimental setup (SNR_{SUN}) were estimated in this study.

SNR was calculated by dividing the mean by the standard deviation of a signal recorded by the instrument. To calculate SNR_{LED}, the HH2 and Spectralon™ white reference panel were set up in the dark room with the LED and a series of 442 measurements were made at one-second intervals. Similarly, SNR_{SUN} was calculated from 600 HH2 observations of the Spectralon™ white reference panel taken in sunlight on a clear day. In each case, the mean and standard deviation of the recorded signals at each wavelength were calculated and the SNR at that wavelength was obtained by dividing the mean by the standard deviation. SNR_{LED} and SNR_{SUN} are the averages of the SNR at each wavelength for each illumination over the full range of measurements (0.325-1.075 μm). These two values were then utilized in estimating the uncertainty of *F*, *SIF*, F_{yield}, and SIF_{yield} values from the HH2 instrument, as outlined in the following paragraph.

F for each plant is taken from the spectrum of the plant under the LED, thus the uncertainty is attributable to the SNR of the instrument. We calculate it for each plant measurement using the following equation:

$$\sigma_F = \frac{F}{SNR_{LED}} \quad (7)$$

where σ_F is the uncertainty of *F*, *F* is fluorescence, and SNR is the signal-to-noise ratio.

Gaussian error propagation on equation (2) is used to characterize the uncertainty in *SIF*. First, the values needed to calculate *SIF*, E_{off}, E_{on}, L_{off}, and L_{on}, values "on" and "off" the absorption band taken from the incoming irradiance spectrum and plant spectrum, respectively, are divided by SNR_{SUN} in order to estimate the instrument uncertainty. Then, by applying a Gaussian error propagation utilizing the uncertainties from the above equations and E_{off}, E_{on}, L_{off}, and L_{on}, and simplifying, we get

$$\sigma_{SIF} = \sqrt{\sigma_{E_{off}}^2 \left(\frac{E_{on} L_{on}}{(E_{off} - E_{on})^2} \right)^2 + \sigma_{E_{on}}^2 \left(\frac{E_{off} L_{off}}{(E_{off} - E_{on})^2} \right)^2 + \sigma_{L_{off}}^2 \left(\frac{E_{on}}{E_{off} - E_{on}} \right)^2 + \sigma_{L_{on}}^2 \left(\frac{E_{off}}{E_{off} - E_{on}} \right)^2} \quad (8)$$

Since an additional calculation is required for the calculations of F_{yield} and SIF_{yield}, we account for the uncertainty propagating through the division by APAR as follows:

Preprints (www.preprints.org) | NOT PEER-REVIEWED | Posted: 24 October 2017 doi:10.20944/preprints201710.0156.v1

$$\sigma_{F_{yield}} = F_{yield}\sqrt{\left(\frac{\sigma_F}{F}\right)^2 + \left(\frac{\sigma_{APAR}}{APAR}\right)^2}$$

$$\sigma_{SIFyield} = SIF_{Yield}\sqrt{\left(\frac{\sigma_{SIF}}{SIF}\right)^2 + \left(\frac{\sigma_{APAR}}{APAR}\right)^2} \quad (9)$$

3. Results

3.1. Fluorescence

Under laboratory conditions, two different LEDs were employed to provide illumination in the PAR range. While these LEDs provide ample radiation in the PAR range, a potential concern is their emission in or near the Oxygen-A band, where we wished to make direct measurements of *F* as described above. **Figure 4** shows the spectra of the two LEDs, 2.2 and 7 W, illuminating the Spectralon white reference panel. As seen in the inset of **Figure 4**, the fluorescence range (0.680-0.78 μm) is relatively unpolluted by the 2.2 W LED, but 0.680-0.720 μm in the PSII range and near the O_2B band, contains some emission from the 7 W LED.

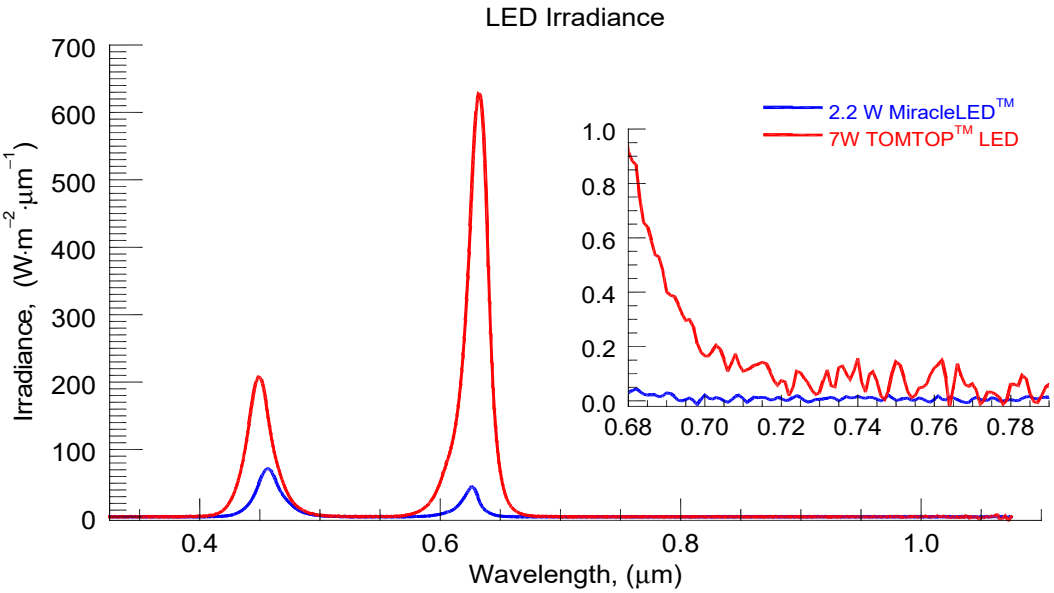

Figure 4. Plot of 2.2 W and 7 W LED grow lamps. Inset: zoom in to the fluorescence range from 0.680-0.780μm.

Under the 2.2 W LED, (**Figure 5**, left panel) both the PSI and PSII peaks are exposed for ivy and fern, showing the full spectrum of *F*. The emission of lilyturf in the PSII region is low and indistinguishable from the noise, but emission in the PSI peak is distinguishable. The ivy, lilyturf, fern and white reference spectra under the 7 W LED illumination are shown in the right panel of **Figure 5** and all three plants have clear emission peaks in the PSI range, where the O_2A band is marked. However, the PSII region and corresponding O_2B band are polluted by the incoming illumination. The pollution of the PSII region, which contains the O_2B band, along with the results of previous studies with instruments of similar spectral resolution [11, 20, 21], justifies limiting our analyses to the O_2A band (*F* at 0.761 μm) for this study.

Preprints (www.preprints.org) | NOT PEER-REVIEWED | Posted: 24 October 2017 doi:10.20944/preprints201710.0156.v1

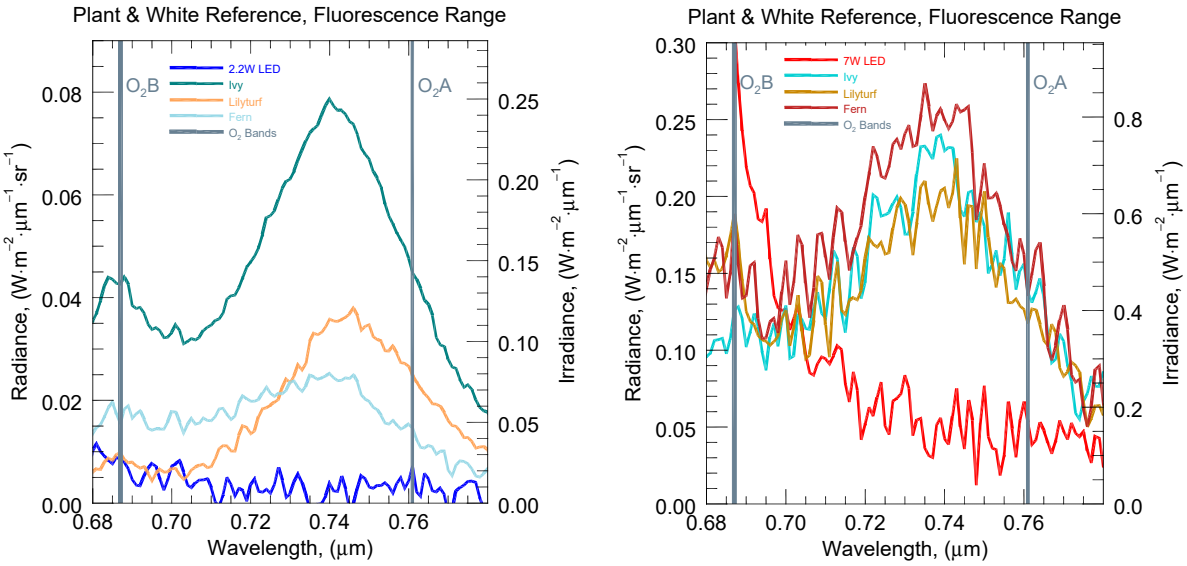

Figure 5. Plot of white reference (incoming irradiance (E_i)) spectra of LEDs and a sample of plant spectra under LED illumination in the fluorescence range (0.680-0.780 µm). The Oxygen-A (O_2A, 0.761 µm) and Oxygen-B (O_2B, 0.687 µm) bands are marked. Not marked are the peaks associated with PSI (near O_2A band) and PSII (near O_2B band). Left: Plants and white reference under the 2.2W LED. Right: Plants and white reference under the 7 W LED.

3.2. Solar induced fluorescence

Unlike the laboratory measurements, *SIF* must be retrieved from within the narrow atmospheric windows where sunlight is absorbed by atmospheric oxygen. A plot of the reference panel spectrum and three vegetation target spectra with the O_2A and O_2B bands marked are shown in **Figure 6**, and **Figure 7** shows the O_2A band more closely. The narrower O_2B band is relatively shallow, indicating the HH2 resolves the wider O_2A band more clearly, as mentioned previously. This result provides additional justification to focus on the O_2A band (0.761 µm) as estimates of *F* and *SIF* for testing our methods.

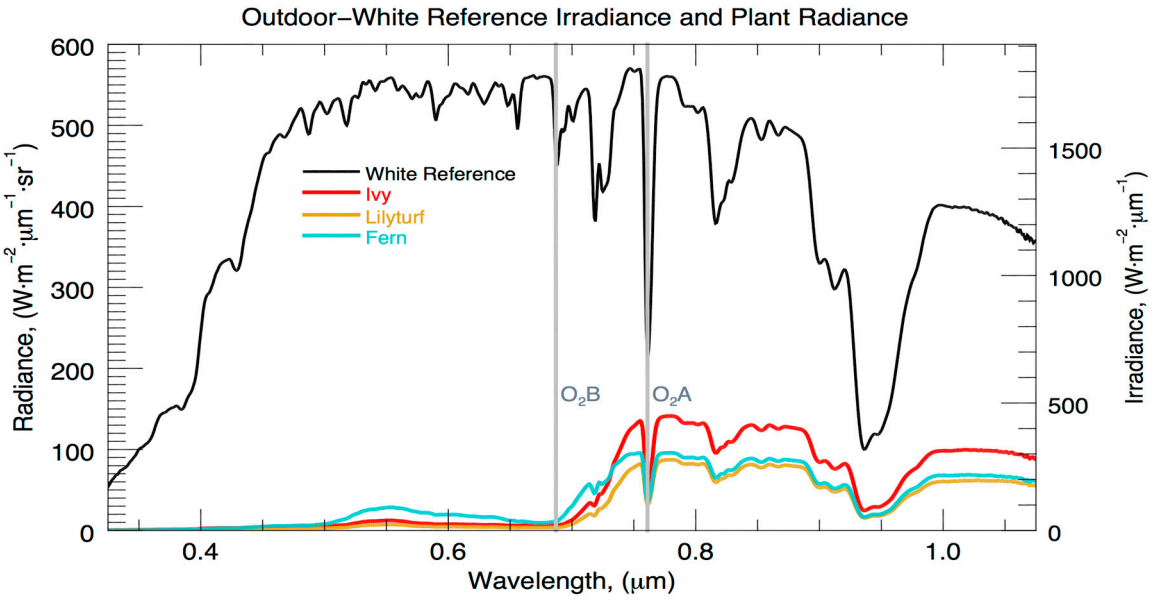

Preprints (www.preprints.org) | NOT PEER-REVIEWED | Posted: 24 October 2017 doi:10.20944/preprints201710.0156.v1

Figure 6. Spectrum of sample plants and white reference measured with ASD HH2 in sunlight. The O_2A and O_2B bands are marked.

In order to estimate *SIF* within the O_2A band, the FLD retrieval method relates the incoming irradiance to the plant target radiance both within the oxygen absorption band and on the shoulder of this spectral feature. **Figure 7** shows the O_2A region of a white reference measurement and plant targets with the λ_{off} -λ_{on} marked for the FLD method. Also illustrated in **Figure 7**, 0.756 μm was chosen as λ_{off} due to its position on the shoulder and 0.761 μm was chosen as the λ_{on} band based on its position in the trough. The assumptions made when using the FLD method include assuming a constant reflectance across the shoulders of the band and neglecting variations in fluorescence. This introduces some error because these two quantities vary across the *SIF* region.

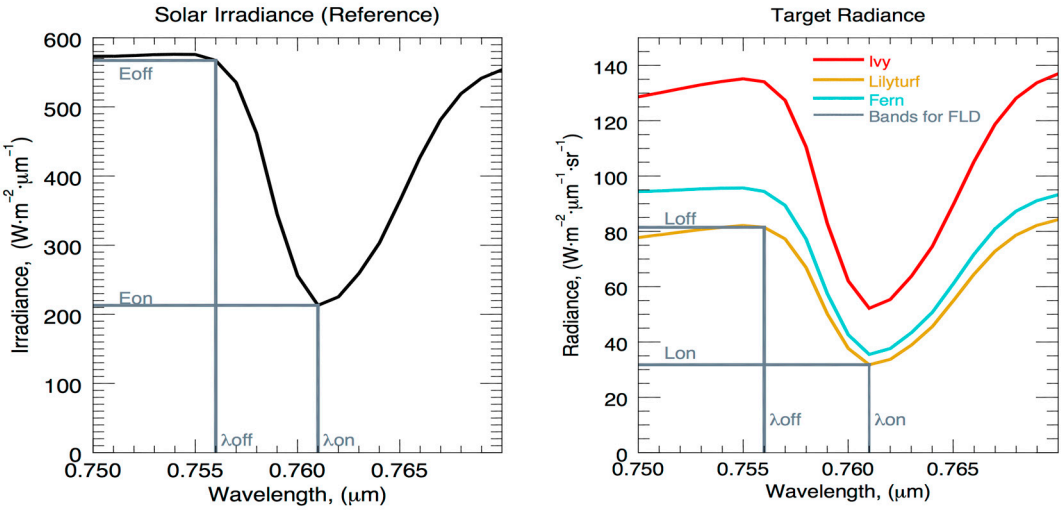

Figure 7. Plot of radiance vs. wavelength near absorption bands with the radiances and wavelengths indicated for FLD method to estimate *SIF*.

3.3. APAR estimates

As outlined in section 2.4, $APAR_\alpha$ and $APAR_\delta$ were calculated for each plant target. To compare the estimates of APAR calculated with the two methods, a separate plot of $APAR_\alpha$ vs. $APAR_\delta$ under LED and under sun for each observation was generated. The results are shown in **Figure 8**. As seen in the top panel of **Figure 8**, the LED based observations show that the values fall just below the 1:1 line and are in good agreement of one another (r=0.99). Average $APAR_\delta$ values were about 12% larger than $APAR_\alpha$. The relationship between $APAR_\alpha$ and $APAR_\delta$ for solar insolation observations falls just below the 1:1 line similar to the LED illuminated measurements and the $APAR_\delta$ method resulted in the average of the values about 22% larger than the $APAR_\alpha$ method under the sun. However, APAR values under the LED maintain a relationship closer to 1:1 than do those in sunlight. In both lighting conditions, LED and sun, the effects of using constant fPAR and one white reference measurement for a set of plant observations to calculate $APAR_\alpha$ result in groups of plant targets having the same value for $APAR_\alpha$. In contrast, the $APAR_\delta$ values vary, even where the same white reference measurement was used for a set of plant targets. We argue that the $APAR_\delta$ method better captures the variation in APAR than when fPAR is treated as a constant as in the $APAR_\alpha$ method. What cannot be separated in the $APAR_\delta$ method is the potential loss of incoming irradiance to the background of the plant and reflected radiance from the plant that misses the detector. We assume that we capture all incoming irradiance, E_i, and the plants absorb a portion and reflect the remainder to the detector. It is reasonable to say that there is radiation that would escape to the background and radiance escaping past the detector to the atmosphere would have us underestimate L_{PAR} and overestimate $APAR_\delta$. We think the magnitude of this radiation not captured

Preprints (www.preprints.org) | NOT PEER-REVIEWED | Posted: 24 October 2017 doi:10.20944/preprints201710.0156.v1

in the measurement is small compared to the magnitude of the measured radiation, thus would have a minimal effect.

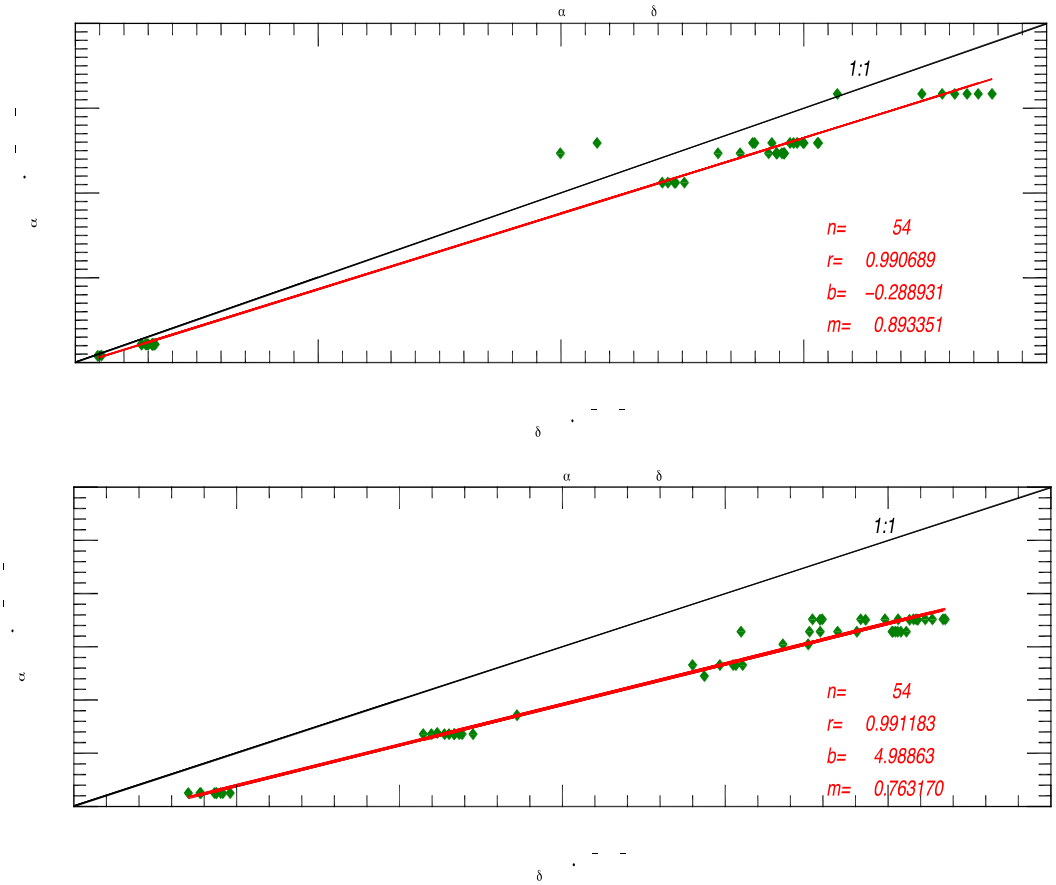

Figure 8. Plot of APAR$_\alpha$ vs APAR$_\delta$ calculated for all plant targets in the study. Top panel: Plant measurements under solar illumination. Bottom panel: measurements under LED.'n': Number of data points. 'r': Correlation coefficient. 'b': bias, 'm' : slope of the linear regression line.

In **Figure 9** we plot *F* (top panel) and *SIF* (bottom panel) against APAR$_\alpha$ (red triangles) and APAR$_\delta$ (blue dots). We see the expected correlation between *F* (or *SIF*) and APAR due to the fact that these quantities are heavily influenced by incoming irradiance. **Figure 9** shows there is a correlation between *F* and APAR as well as *SIF* and APAR, using both the APAR$_\alpha$ and APAR$_\delta$ methods. In both panels of **Figure 9**, The APARα values, indicated by red triangles, are grouped together due to the use of one white reference measurement used for a set of plant targets and the assumption that fPAR is constant. In contrast, APAR$_\delta$ (blue circles) values vary along the APAR axis despite also utilizing the same white reference measurements for sets of plant target, confirming our expectation that fPAR varies for different plants. Utilizing this result, we concluded that APAR$_\delta$ would be used in subsequent portions of the study. Figure 10 (top panel) also shows clustering indicative of the difference in power between the two LEDs along the x-axis and much lower *F* values for the lower Power LED, which illustrates that the power of the illumination, and thus APAR value, strongly influences *F* values. **Figure 9** (bottom) shows *SIF* and APAR are also positively correlated, indicating that *SIF* is driven higher when APAR increases. These results would be consistent with a plant increasing fluorescence if the incoming radiation increases. These results again support the expectation that APAR is heavily influential on *F* and *SIF*, as expected from the literature, but additionally show we can estimate *F* and *SIF* passively with sufficient accuracy to capture this relationship. Although the correlation is weaker for *SIF* than *F* when plotted against APAR$_\delta$, both correlations are important in this study to provide a basis for showing we can account for the

Preprints (www.preprints.org) | NOT PEER-REVIEWED | Posted: 24 October 2017 doi:10.20944/preprints201710.0156.v1

394 influence of APAR on *F* and *SIF* when calculating F_{yield} and SIF_{yield}. Of further significance in **Figure 9**
395 is the difference in the range of *F* and *SIF* values which are around one order of magnitude, again
396 demonstrating the heavy influence of APAR on *F* and *SIF*.
397

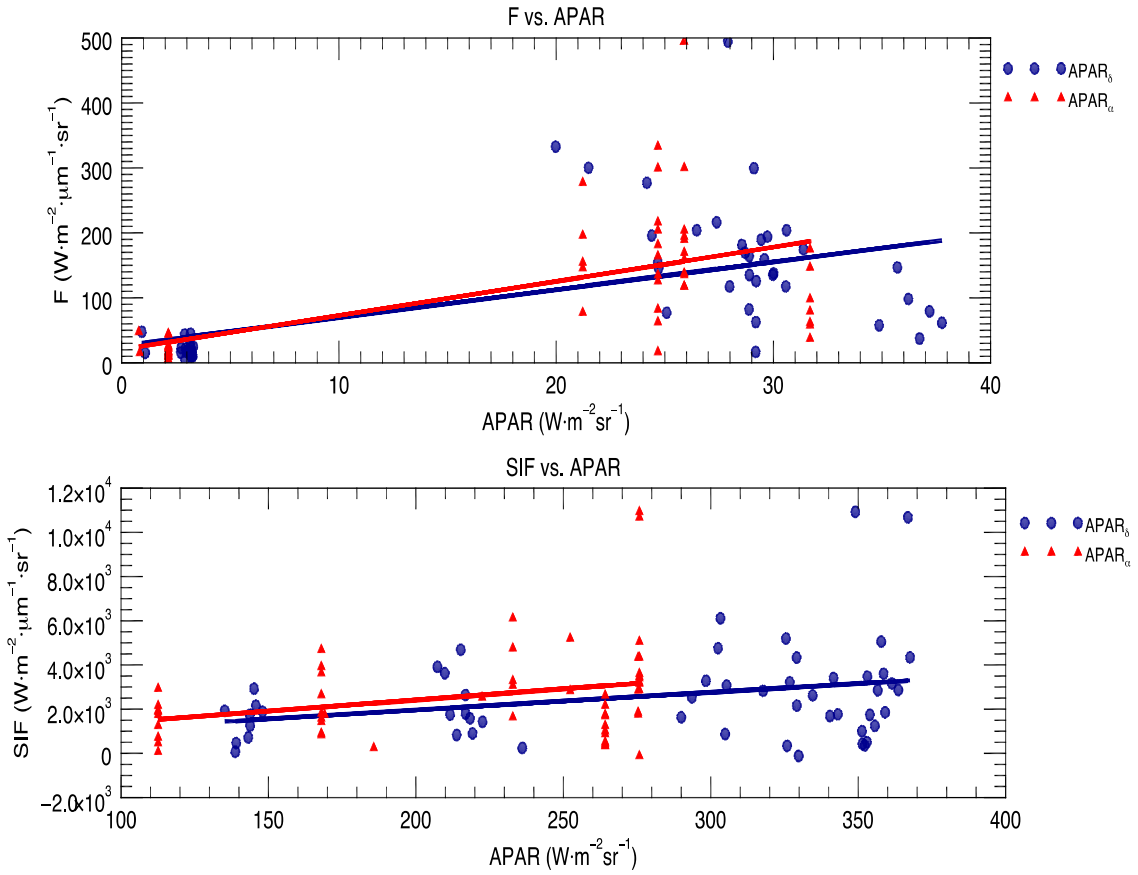

398
399
400 **Figure 9. Fluorescence and solar induced fluorescence for plants in the study. $APAR_{\delta}$ values are**
401 **represented by blue circles and $APAR_{\alpha}$ represented by red triangles. Top: F for all plants in the**
402 **study versus APAR estimates from both techniques. Bottom: *SIF* for all plant targets in the study**
403 **versus APAR for both techniques used.**

404 *3.4.Fluorescence yield and solar induced fluorescence yield estimates*

405 The resulting estimates of F_{yield} are plotted against $APAR_{\delta}$ are shown in **Figure 10** (top). When
406 compared to the correlation between *F* and $APAR_{\delta}$ shown in **Figure 9** (top), the relationship
407 disappears entirely for F_{yield} and $APAR_{\delta}$ (**Figure 10**, top panel). Similarly, the values obtained for
408 SIF_{yield} are plotted against $APAR_{\delta}$ in **Figure 10** (bottom). Although the correlation between *SIF* and
409 $APAR_{\delta}$ (**Figure 9**, bottom panel) was weaker than for F, the relationship that did exist was removed
410 by the normalization calculation. In fact, if it were not for the effect of a suspected outlier, the small
411 relationship appearing in **Figure 10** would have disappeared entirely. Since we were utilizing a
412 relatively small dataset (n=54) to test these methods, it was decided not to exclude this suspected
413 outlier at this time.
414

Preprints (www.preprints.org) | NOT PEER-REVIEWED | Posted: 24 October 2017 doi:10.20944/preprints201710.0156.v1

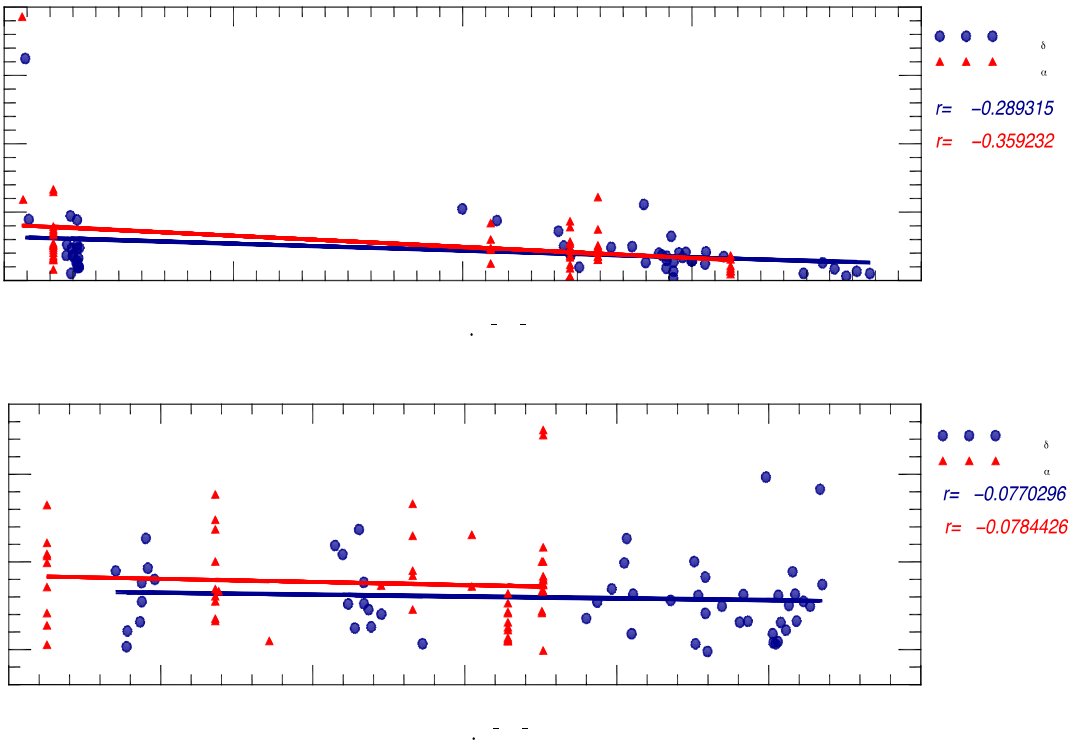

Figure 10. Fluorescence yield (F_{yield}) and solar induced fluorescence yield (SIF_{yield}) values versus absorbed photosynthetically active radiation. Both methods of estimating APAR, $APAR_{\delta}$ and $APAR_{\alpha}$, blue and red respectively, are included. Top: F_{yield} versus APAR. Bottom: SIF_{yield} versus APAR.

3.5. Fluorescence uncertainty

Spectral SNR under the LED (see Section 2.5) for this experiment shown in **Figure 11** illustrates the overall pattern of SNR for the wavelength range in the LED environment. When the average of these spectral SNR data are taken, the resulting SNR_{LED} is 18.6, which corresponds to a relative error of 5.4% for measurements of *F*. This value differs from the manufacturer's SNR of 6659.1 (0.02% relative error) due to the difference in the illumination in the two conditions. The large difference in these two values supports the need for examination instrument and other contributing uncertainty for the two illumination sources. Using the manufacturer's reported SNR data would have underestimated the uncertainty in the estimates of *F* in this study. It was expected that uncertainty estimated from LED observations would be larger compared to the calibrated light source, due to the LED not being calibrated, the relatively low power of the LED, and the limited number of wavelengths emitting radiation. The value obtained for SNR_{LED} was utilized in Equation 7 to get the uncertainty of estimates of *F*. The variation in the data observed from these experiments is much larger than the instrument error. This suggests that variations in illumination or other environmental variables are the main source of error at least when compared to instrumental error.

Arguably, from Figure 5, measurements of fluorescence will yield a slightly better SNR than the white reference illuminated with the LED because fluorescence emission is about a factor of four to five higher than the remaining contamination by the LED emission. Therefore, a value of around 20 for the SNR also appears to be justified in the fluorescence range. This value would also be visually comparable to the spectral noise visible in the three plant spectra shown in Figure 5, right panel.

Preprints (www.preprints.org) | NOT PEER-REVIEWED | Posted: 24 October 2017 doi:10.20944/preprints201710.0156.v1

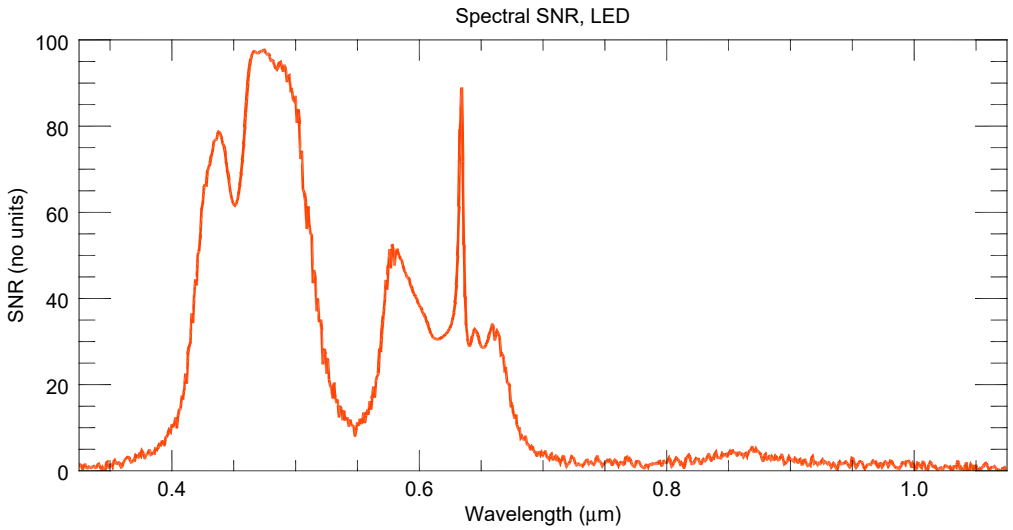

Figure 11. Plot of spectral SNR for the LED and Spectralon® white reference panel (n=442).

3.6. Solar induced fluorescence uncertainty

Using the methods described in Section 2.5 we calculate SNR_{SUN} of the instrument as 158.9, which is a relative error of 0.63% for 600 observations made in sunlight using the HH2. The average solar spectral SNR plot is shown in **Figure 12**. When compared to the manufacturer's estimate of SNR for the HH2 of 6659.1 (0.02% relative error), the relative error is higher under sunlight . This is likely due largely to the difference in illumination sources between the calibrated source used by ASD and sunlight. While every effort was made to control the environment during the SNR experiments, the data collected were affected by variations in detected illumination from the sun and atmosphere. Additionally, the difference in the power of the sources affects the outcome. It was anticipated that the relative error would be greater in the case of the solar experiment due to conditions being less controlled. Because our study involves a comparison of extreme lighting conditions in experiments that differ from calibration conditions, these results support the need for this independent assessment of SNR as well as the propagation of uncertainty through the next steps of the study (Section 2.5).

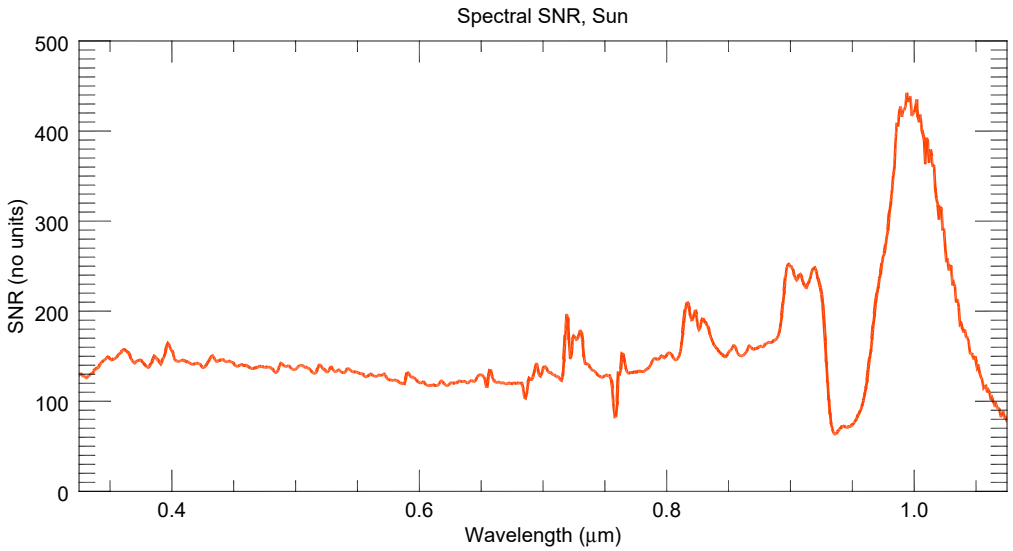

Figure 12. Plot of solar spectral SNR using the Spectralon white reference panel (n=600).

Preprints (www.preprints.org) | NOT PEER-REVIEWED | Posted: 24 October 2017 doi:10.20944/preprints201710.0156.v1

3.7. Comparing CF metrics

Employing the uncertainty associated with each fluorescence metric, we calculated the averages and propagated uncertainties of *F*, *SIF*, F_{yield}, and SIF_{yield}. Average values for *F* and *SIF* for all plants in the experiment are shown in the top row **Table 1**. *F* and *SIF* are different by a factor of approximately 24, clearly outside the margin of error of one another. This result was expected due to the vastly different lighting environments constructed for the study. We also expected to sufficiently account for the influence of incoming irradiance and APAR when calculating F_{yield} and SIF_{yield} such that we would be able to generate comparable values F_{yield} and SIF_{yield}. The bottom row of **Table 1** contains the normalized fluorescence estimates, F_{yield} and SIF_{yield}, which are within the margin of error of one another. This result is consistent with the hypothesis that the plant fluorescence yield is linearly related to APAR. The values we obtained with these methods for all of the CF metrics calculated are comparable to the literature (e.g. [18, 41-45]). It further demonstrates the suitability of our methods of estimating the fluorescence metrics and accounting for APAR to a degree that can be utilized in future studies of the response of plants to stress or comparisons of photosynthetic differences due to physiological characteristics, for instance.

Table 1. Average fluorescence, fluorescence yield, solar-induced fluorescence, and solar-induced fluorescence yield for plant target measurements. All plant targets are listed in Table A 1.

	F **n=54**	**SIF** **n=54**
Including APAR **($Wm^{-2}\mu m^{-1}sr^{-1}$)**	0.110±0.006	2.60±1.87
Yield **(no units)**	0.022±0.001	0.030±0.020

The estimates of uncertainty shown in **Table 1** are a result of the methods outlined in Section 2.5. These uncertainties result in relative error of 5.5% for *F* values and slightly better at 4.5% for F_{yield} values. While these relative errors are larger than the relative error of approximately 0.05% reported by the manufacturer, we accounted for the SNR of the instrument, variations in incoming radiation, and other noise sources uniquely through the SNR experiments. The relative error of *SIF* and SIF_{yield} were 72% and 67%, respectively. It was expected that these relative errors would be larger due to the calculated SNR for the HH2 in sun, also a non-calibrated light source, being propagated through the FLD retrieval.

4. Discussion

Employing LED's in the dark tent allow us to see *F* over the majority of the chlorophyll fluorescence (CF) range with little interference from incoming irradiance from the source. The 2.2 W LED contributed less pollution to this range than the 7 W LED in the 0.680-0.720 μm range, which corresponds to the PSII portion of CF. This and the relatively shallow trough of the corresponding atmospheric O_2B band in this region led us to focus on the portion of the CF spectrum around the O_2A band, or the PSI peak. Furthermore, only one wavelength in the PSI region, 0.761 μm, was selected for examination in this study. Thus, further studies utilizing or examining the information that might be contained in the full spectrum are needed.

Results of *SIF* retrievals from the HH2 showed reliable estimates of this metric can be obtained from a variety of plants utilizing the FLD method. We show *SIF* values comparable to the literature (e.g. [18, 42]) can be obtained with the HH2, even when uncertainty estimates are maximized. While spectrometers with higher resolution and smaller sampling interval improve SNR, we show evidence that a more precise instrument may not improve *F* or *SIF* estimates. To address this question, isolation and control for various sources of environmental variability is needed. With this in mind, we propose that comparison studies of *SIF* and SIF_{yield} should be undertaken with passive

Preprints (www.preprints.org) | NOT PEER-REVIEWED | Posted: 24 October 2017 doi:10.20944/preprints201710.0156.v1

spectroscopy, even with the HH2, to better understand how *SIF* and SIF_{yield} link to other parameters, such as LUE and GPP. Additionally, time series analyses of SIF and/or SIFyield would potentially reveal the response of plants to environmental changes or stresses. Additionally, we suggest further investigations into improving upon these results. For instance, enhanced versions of the FLD method, spectral fitting methods, or other approaches may improve the SIF retrievals [18, 22, 46-52] by reducing relative error.

We tested two methods of estimating the absorbed photosynthetically active radiation (APAR) from spectral measurements, $APAR_{\alpha}$ and $APAR_{\delta}$. We chose to utilize the $APAR_{\delta}$ technique to calculate F_{yield} and SIF_{yield} because this accounted for unique fPAR for plant targets, while the $APAR_{\alpha}$ method does not. The $APAR_{\delta}$ method does, however, neglect the small contribution of CF photons to the PAR region approximately 0.680-0.700μm. Future studies using this technique may address this issue by estimating the contribution or determining the uncertainty that neglecting CF photons introduces. While the $APAR_{\delta}$ method accounts more uniquely for the use of incoming radiation by plants than the $APAR_{\alpha}$ method, the $APAR_{\delta}$ method may not fully account for irradiance lost to the background or reflected radiance amounts that do not reach the sensor. This lost energy is included in the $APAR_{\delta}$ value, yet are not really absorbed by the plant. These two sources of uncertainty in $APAR_{\delta}$ may or may not be accounted for in the $APAR_{\alpha}$ method. Despite our choice in the study to focus on $APAR_{\alpha}$, both methods of estimating APAR remain interesting and further study of their differences and the factors affecting the values is warranted.

Average F_{yield} and SIF_{yield} for this set of plant targets using these techniques were within the margin of error of one another and are comparable to the literature (e.g. [41, 43, 53]. The comparability of F_{yield} and SIF_{yield} estimates in this study points to the usefulness of the observations made with the HH2 to estimate fluorescence metrics and APAR. While a direct correlation between estimates of *F* and *SIF* or between F_{yield} and SIF_{yield} for each individual plant could not be established under the conditions of these experiments, our ability to account for incoming irradiance between the two extreme illumination conditions is very promising. With more rigorous controls on environmental conditions and a measurement protocol that could cut down the time between observations, there is the potential to use these two experimental setups in tandem to search for more quantitative links between full spectrum *F* and retrievals of *SIF* derived from passive measurements. These links could then be exploited for upscaling to multi-plant, canopy, or regional scales. We utilized a relatively limited dataset to test the techniques presented, but propose that collecting data over a more continuous range of APAR either in the laboratory, in the field, or both, could potentially reveal more detailed relationships regarding chlorophyll fluorescence.

5. Conclusions

This study describes the use of a passive spectroradiometer to estimate *F* and *SIF* and account for APAR in radiance units and to sufficiently estimate F_{yield} and SIF_{yield}. We provide a basis for subsequent studies using both laboratory and outdoor experimental setups in conjunction or separately to further explore fluorescence, photosynthesis, GPP, and other quantities. In particular, we show that fluorescence yield can be estimated from concurrent APAR and plant spectral measurements even under extreme lighting conditions. Currently, there are gaps in understanding and scaling photosynthetic processes that active measurements cannot address. It is in this context that passive spectroscopy can play a role. Additionally, the relationships of interest among fluorescence metrics, photosynthesis, and GPP remain poorly explained, but desirable to examine regional photosynthetic activity between plant communities. Employing methods Utilizing passive observations of F and SIF to explore their specific relationships to gross primary production parameters and underlying photosynthetic processes in future studies would open up opportunities to upscale and compare measurements from different experiments.

Employing LEDs in the laboratory provide a low-cost opportunity to examine plant-scale responses of fluorescence by lower-cost, passive means, thus a basis for exploring quantities of interest in botany, ecology, agriculture, and remote sensing. The normalizing method applied to *SIF* at these scales is a potential next step to relating *SIF* and gross primary production, possibly by

Preprints (www.preprints.org) | NOT PEER-REVIEWED | Posted: 24 October 2017 doi:10.20944/preprints201710.0156.v1

552 disentangling light use efficiency of photosynthesis and fluorescence or getting at the
553 structure-related escape probability of fluorescence photons for increasingly complex vegetation [6,
554 17, 54, 55]. Quantities such as LUE and escape probability are often assumed to be constants in
555 current modeling studies and are found to be too complex to address in the field without further
556 study. Most studies have required additional measurements from additional instruments mounted
557 on flux towers or other platforms to compare fluorescence metrics and explore relationships to
558 APAR and environmental conditions [6, 56-59]. By contrast, our methods may prove translatable to
559 areas where flux towers and other instrumentation are not available, thus increasing the spatial
560 extent over which we can search for relationships among *SIF*, SIF_{yield} and GPP parameters, such as
561 LUE, as well as continue progress toward a better understanding of the SIF-GPP relationship.
562 Further application of this method in experimental, modeling, and remote sensing studies could
563 lead to improved estimates for different plant functional groups, i.e. different photosynthetic
564 pathways, as well as a determination of relative differences in photosynthetic activity by land-cover
565 type. The techniques presented here can be utilized as a basis for new protocols in field studies in
566 remote locations. Our *SIF* estimates made with an untethered passive instrument give researchers
567 the opportunity to add many CF datasets from an increased number of study areas to the current
568 body of values available.
569

570 **Acknowledgments:** This work was supported by a grant partnership between Vanderbilt University
571 and the São Paulo Research Foundation (FAPESP), as well as a Vanderbilt College of Arts & Sciences
572 Research Grant. The authors thank Siobhan Fathel, Rodrigo Nunes, David Furbish, Kristy Barnes,
573 Marty Martinez, Dan Gorzinsky, Tyler Doane and Jennifer Bradham for their support, valuable
574 contributions, and discussions.
575

576 **Author Contributions:** T. Merrick designed and conducted the experiments with the assistance of
577 R. Bennartz, and developed the code with assistance from J. Rausch and R. Bennartz. G. Gualda and
578 R. Bennartz guided the error propagation. R. Bennartz oversaw the normalization development and
579 coding. M.L.S.P Jorge and Thiago S.F. Silva provided data analysis and statistics for the project as
580 well as guidance in the fields of biology and ecology. T. Merrick prepared the manuscript with
581 contributions from all authors.

582 **Conflicts of Interest:** The authors declare no conflict of interest.

583 **Appendix A**

584 **Table A 1. A table of nomenclature for the study.**

Nomenclature	
APAR	Absorbed Photosynthetically Active Radiation
$APAR_{\alpha}$	Absorbed Photosynthetically Active Radiation using fPAR estimate from literature
$APAR_{\delta}$	Absorbed Photosynthetically Active Radiation using difference between incoming/reflected spectra
E	Spectral Irradiance [$Wm^{-2}\mu m^{-1}$]
E_i	Incoming spectral Irradiance [$Wm^{-2}\mu m^{-1}$]
E_{off}	Spectral Irradiance off oxygen band; at shoulder [$Wm^{-2}\mu m^{-1}$]
E_{on}	Spectral Irradiance on oxygen band; at the trough [$Wm^{-2}\mu m^{-1}$]
F	Fluorescence under illumination other than sun; F under LED [$Wm^{-2}\mu m^{-1}\,sr^{-1}$]
FLD	Fraunhofer Line Depth Method
fPAR	Fraction Absorbed Photosynthetically Active Radiation
FWHM	Full Width-Half Maximum
F_{yield}	Fluorescence Yield; Fluorescence Quantum Yield [no units]
GPP	Gross Primary Production

Preprints (www.preprints.org) | NOT PEER-REVIEWED | Posted: 24 October 2017 doi:10.20944/preprints201710.0156.v1

HH2	ASD Handheld 2 Pro Spectroradiometer
L	Spectral Radiance [$Wm^{-2}\mu m^{-1} sr^{-1}$]
LED	Light Emitting Diode
L_{off}	Spectral Radiance off oxygen band; at shoulder [$Wm^{-2}\mu m^{-1} sr^{-1}$]
L_{on}	Spectral Radiance on oxygen band; at the trough [$Wm^{-2}\mu m^{-1} sr^{-1}$]
L_{PAR}	Reflected Radiance from plant 0.400-0.700µm range [$Wm^{-2}\mu m^{-1} sr^{-1}$]
LUE	Light Use Efficiency
O_2A	Oxygen-A band; Center at 761nm in this study
O_2B	Oxygen-B band; Center at 687nm in this study
PAM	Pulse Amplitude Modulation fluorimetry
PAR	Photosynthetically Active Radiation
PSI	Photosystem I
PSII	Photosystem II
R	Reflectance [no units]
SIF	Solar-induced Fluorescence [$Wm^{-2}\mu m^{-1} sr^{-1}$]
SIF_{off}	Solar-induced Fluorescence off oxygen band; at shoulder [$Wm^{-2}\mu m^{-1} sr^{-1}$]
SIF_{on}	Solar-induced Fluorescence on oxygen band; at the trough [$Wm^{-2}\mu m^{-1} sr^{-1}$]
SIF_{yield}	Solar-induced Fluorescence Yield [no units]
SNR	Signal-to-Noise Ratio
SNR_{LED}	Signal-to-Noise Ratio calculated for LED
SNR_{sun}	Signal-to-Noise Ratio calculated for sunlight
λ	Wavelength of Radiation [µm]
σ	Standard Deviation

585
586

Preprints (www.preprints.org) | NOT PEER-REVIEWED | Posted: 24 October 2017 doi:10.20944/preprints201710.0156.v1

Table A 2. Plants used in the study and brief characteristics.

Plant	Type	Size	Sample Location/Type	Density
GRASS	Natural	clipped	lawn	dense
KENTUCKY COFFEE TREE	Natural	small	fragment	medium
AMERICAN CHESTNUT	Natural	medium	fragment	medium
SUGAR MAPLE	Natural	medium	fragment	medium
CEDAR	Natural	medium	secondary growth	medium
CLOVER	Natural	tall	trail edge	medium
FESCUE	Natural	tall	trail edge	dense
PAMPAS GRASS	Natural	medium	landscaping	dense
SPRUCE	Natural	small	landscaping	healthy
IVY	Natural	dense	landscaping	healthy
MAPLE	Natural	large	landscaping	healthy
DOGWOOD	Natural	large	landscaping	healthy
EVERGREEN	Natural	short	landscaping	dense
HOLLY	Natural	large	landscaping	dense
PINE	Natural	large	landscaping	medium
VARIEGATED LILY TURF	Natural	small	landscaping	dense
MAGNOLIA	Natural	large	landscaping	dense
PEPPER	Potted	small	houseplant	sparse
TOMATO	Potted	small	houseplant	sparse
SPRUCE	Potted	small	houseplant	sparse
PINE	Potted	small	houseplant	sparse
HEN & CHICKEN	Potted	small	houseplant	dense
IVY-1	Potted	small	houseplant	sparse
GREEN LILY TURF	Potted	small	houseplant	medium
SMALL FERN	Potted	small	houseplant	sparse
ANTHURIUM	Potted	small	houseplant	sparse
RED AGLAONEMA	Potted	large	houseplant	dense
FOUNTAINGRASS	Potted	medium	houseplant	medium
IVY	Potted	small	houseplants	sparse
VARIEGATED LILY TURF	Potted	medium	houseplant	dense
SWEDISH IVY	Potted	small	houseplant	medium
AEONIUM	Potted	small	houseplant	dense
POTHOS	Potted	medium	houseplant	dense
LARGE FERN	Potted	medium	houseplant	medium
JANET CRAIG	Potted	large	houseplant	dense
MOTHER IN LAWS TONGUE	Potted	large	houseplant	dense
SPIDER	Potted	medium	houseplant	dense

Literature Cited

1. Tschiersch, H., et al., *Establishment of integrated protocols for automated high throughput kinetic chlorophyll fluorescence analyses.* Plant Methods, 2017. **13**: p. 54.
2. Fiorani, F., et al., *Imaging plants dynamics in heterogenic environments.* Curr Opin Biotechnol, 2012. **23**(2): p. 227-35.

3. Rossini, M., et al., *Red and far-red sun-induced chlorophyll fluorescence as a measure of plant photosynthesis.* Geophysical Research Letters, 2015: p. n/a-n/a.
4. Damm, A., et al., *Far-red sun-induced chlorophyll fluorescence shows ecosystem-specific relationships to gross primary production: An assessment based on observational and modeling approaches.* Remote Sensing of Environment, 2015. **166**: p. 15.
5. Damm, A., et al., *Impact of varying irradiance on vegetation indices and chlorophyll fluorescence derived from spectroscopy data.* Remote Sensing of Environment, 2015. **156**: p. 202-215.
6. Damm, A., et al., *Remote sensing of sun-induced fluorescence to improve modeling of diurnal courses of gross primary production (GPP).* Global Change Biology, 2010. **16**(1): p. 171-186.
7. Baker, N.R., *Chlorophyll fluorescence: a probe of photosynthesis in vivo.* Annu Rev Plant Biol, 2008. **59**: p. 89-113.
8. Campbell, P.K., et al., *Contribution of chlorophyll fluorescence to the apparent vegetation reflectance.* Sci Total Environ, 2008. **404**(2-3): p. 433-9.
9. Magney, T.S., et al., *Connecting active to passive fluorescence with photosynthesis: a method for evaluating remote sensing measurements of Chl fluorescence.* New Phytol, 2017.
10. Liu, L., et al., *Assessing photosynthetic light-use efficiency using a solar-induced chlorophyll fluorescence and photochemical reflectance index.* International Journal of Remote Sensing, 2013. **34**(12): p. 4264-4280.
11. Flexas, J., et al., *Steady-state chlorophyll fluorescence (Fs) measurements as a tool to follow variations of net CO2 assimilation and stomatal conductance during water-stress in C3 plants.* PHYSIOLOGIA PLANTARUM, 2002. **114**: p. 10.
12. Porcar-Castell, A., et al., *Linking chlorophyll a fluorescence to photosynthesis for remote sensing applications: mechanisms and challenges.* J Exp Bot, 2014. **65**(15): p. 4065-95.
13. Kalaji, H.M., et al., *Identification of nutrient deficiency in maize and tomato plants by in vivo chlorophyll a fluorescence measurements.* Plant Physiol Biochem, 2014. **81**: p. 16-25.
14. Kalaji, H.M., et al., *Frequently asked questions about in vivo chlorophyll fluorescence: practical issues.* Photosynth Res, 2014. **122**(2): p. 121-58.
15. Frankenberg, C. *Retrieval of chlorophyll fluorescence from space*. in *KISS Fluorescence workshop*. 2012. Jet Propulsion Laboratory / California Institute of Technology, Pasadena, CA
16. Frankenberg, C., et al., *New global observations of the terrestrial carbon cycle from GOSAT: Patterns of plant fluorescence with gross primary productivity.* Geophysical Research Letters, 2011. **38**(17): p. n/a-n/a.
17. Guanter, L., et al., *Global and time-resolved monitoring of crop photosynthesis with chlorophyll fluorescence.* Proc Natl Acad Sci U S A, 2014. **111**(14): p. E1327-33.
18. Meroni, M., et al., *Remote sensing of solar-induced chlorophyll fluorescence: Review of methods and applications.* Remote Sensing of Environment, 2009. **113**(10): p. 2037-2051.
19. Meroni, M., et al., *Using optical remote sensing techniques to track the development of ozone-induced stress.* Environ Pollut, 2009. **157**(5): p. 1413-20.
20. Gomez-Chova, L., et al., *Solar induced fluorescence measurements using a field spectroradiometer.* AIP Conference Proceedings, 2006. **852**: p. 274-281.
21. Julitta, T., et al., *Comparison of Sun-Induced Chlorophyll Fluorescence Estimates Obtained from Four Portable Field Spectroradiometers.* Remote Sensing, 2016. **8**(2): p. 122.

22. Julitta, T., *Optical proximal sensing for vegetation monitoring*, in *Department of Earth and Environmental Sciences*. 2015, University of Milano-Bicocca. p. 136.
23. Louis, J., et al., *Remote sensing of sunlight-induced chlorophyll fluorescence and reflectance of Scots pine in the boreal forest during spring recovery.* Remote Sensing of Environment, 2005. **96**(1): p. 37-48.
24. Govindjee, G., *"Chlorophyll a fluorescence: a bit of basics and history."* in *Chlorophyll a fluorescence: a signature of photosynthesis*, G.a.G. Papageorgiou, G, Editor. 2004, Springer: Dordrecht. p. 1-42.
25. ASDInc., *FieldSpec® HandHeld 2™ Spectroradiometer User Manual*. 2010, Boulder, CO: ASD, Inc. 93.
26. ASD, I., *FieldSpec 4 User Manual*. 2011, ASD Inc.: Boulder, CO. p. 92.
27. Plascyk, J.A. and F.C. Gabriel, *The Fraunhofer Line Discriminator MKII-An Airborne Instrument for Precise and Standardized Ecological Luminescence Measurement.* IEEE TRANSACTIONS ON INSTRUMENTATION AND MEASUREME, 1975. **IM-24**(4): p. 8.
28. I. Moya, L.C., S. Evain, Y. Goulas, Z.G. Cerovic, G. Latouche, J. Flexas, A. Ounis, *A new instrument for passive remote sensing1. Measurements of sunlight-induced chlorophyll fluorescence.* Remote Sensing of Environment, 2004. **91**(2): p. 186-197.
29. Plascyk, J.A., *The MK II Fraunhofer Line Discriminator (FLD -II) for Airborne and Orbital Remote Sensing of Solar-Stimulated Luminescense.* Optical Engineering, 1975. **14**(4): p. 8.
30. Van Wittenberghe, S., et al., *Upward and downward solar-induced chlorophyll fluorescence yield indices of four tree species as indicators of traffic pollution in Valencia.* Environ Pollut, 2013. **173**: p. 29-37.
31. McCree, K.J., *Test of current definitions of photosynthetically active radiation against leaf photosynthesis data.* Agricultural Meteorology, 1972. **10**: p. 10.
32. Zhang, Y., et al., *Estimation of vegetation photosynthetic capacity from space-based measurements of chlorophyll fluorescence for terrestrial biosphere models.* Glob Chang Biol, 2014. **20**(12): p. 3727-42.
33. Inada, K., *Action spectra for photosynthesis in higher plants.* Plant and Cell Physiology, 1976. **17**: p. 10.
34. McCree, K.J., *The action spectrum, absorptance and quantum yield of photosynthesis in crop plants* Agricultural Meteorology, 1972. **9**: p. 25.
35. Bula, R.J., et al., *Light-emitting diodes as radiation source for plants.* Horticulture Science, 1991. **26**(2): p. 3.
36. Van Wittenberghe, S., et al., *A field study on solar-induced chlorophyll fluorescence and pigment parameters along a vertical canopy gradient of four tree species in an urban environment.* Sci Total Environ, 2014. **466-467**: p. 185-94.
37. Li, Z. and L. Moreau, *A new approach for remote sensing of canopy-absorbed photosynthetically active radiation. I: Total Surface Absorption.* Remote Sensing of Environment, 1996. **55**: p. 16.
38. J.L.Monteith, *Climate and the efficiency of crop production in Britain.* Phil. Trans. R. Soc. Land., 1977. **281**: p. 17.
39. Monteith, J.L., *Solar Radiation and Productivity in Tropical Ecosystems.* Journal of Applied Ecology, 1972. **9**(3): p. 19.

679 40. Damm, A., et al., *Deriving sun-induced chlorophyll fluorescence from airborne based spectrometer*
680 *data.* Proc. 'Hyperspectral 2010 Workshop', Frascati, Italy,17–19 March 2010 (ESA SP-683,
681 May 2010), 2010: p. 7.
682 41. Rascher, U., G. Agati, L. Alonso, G. Cecchi, S. Champagne, R. Colombo, A. Damm, F.
683 Daumard, E. de Miguel, G. Fernandez, B. Franch, J. Franke, C. Gerbig, B. Gioli, J. A. Gomez,
684 Y. Goulas, L. Guanter, O. Gutie rrez-de-la-Camara, K. Hamdi, P. Hostert, M.Jimenez, M.
685 Kosvancova, D. Lognoli, M. Meroni, F. Miglietta, A. Moersch, J. Moreno, I. Moya, B.
686 Neininger, A. Okujeni, A. Ounis, L. Palombi, V. Raimondi, A. Schickling, J. A. Sobrino, M.
687 Stellmes, G. Toci, P. Toscano, T. Udelhoven, S. van der Linden, and A. Zaldei, *CEFLES2: the*
688 *remote sensing component to quantify photosynthetic efficiency from the leaf to the region by*
689 *measuring sun-induced fluorescence in the oxygen absorption bands.* Biogeosciences Discussions,
690 2009. **6**: p. 2217-2266.
691 42. Rossini, M., Alonso, L., Cogliati, S., Damm, A., Guanter, L., Julitta, T., Meroni, M., Moreno,
692 J., Panigada, C., Pinto, F. and Rascher, U. *Measuring sun-induced chlorophyll fluorescence: An*
693 *evaluation and synthesis of existing field data*. in *5th International workshop on remote sensing of*
694 *vegetation fluorescence*. 2014. Paris, France.
695 43. Rossini, M., et al., *Analysis of Red and Far-Red Sun-Induced Chlorophyll Fluorescence and Their*
696 *Ratio in Different Canopies Based on Observed and Modeled Data.* Remote Sensing, 2016. **8**(5): p.
697 412.
698 44. Guanter, L., et al., *Using field spectroscopy to assess the potential of statistical approaches for the*
699 *retrieval of sun-induced chlorophyll fluorescence from ground and space.* Remote Sensing of
700 Environment, 2013. **133**: p. 52-61.
701 45. Cogliati, S., et al., *Continuous and long-term measurements of reflectance and sun-induced*
702 *chlorophyll fluorescence by using novel automated field spectroscopy systems.* Remote Sensing of
703 Environment, 2015.
704 46. Liangyun Liu, X.L., ZhihuiWang, and Bing Zhang, *Measurement and Analysis of*
705 *BidirectionalSIF Emissions in Wheat Canopies.* IEEE TRANSACTIONS ON GEOSCIENCE
706 AND REMOTE SENSING, 2016: p. 12.
707 47. Liu, X. and L. Liu, *Improving Chlorophyll Fluorescence Retrieval Using Reflectance Reconstruction*
708 *Based on Principal Components Analysis.* IEEE GEOSCIENCE AND REMOTE SENSING
709 LETTERS, 2015(Accepted for publication).
710 48. Luis Alonso, L.G.-C., Joan Vila-Francés, Julia Amorós-López, Luis Guanter, Javier Calpe,
711 and José Moreno, *Improved Fraunhofer Line Discrimination Method for Vegetation Fluorescence*
712 *Quantification.* IEEE GEOSCIENCE AND REMOTE SENSING LETTERS, 2008. **5**(4): p. 5.
713 49. Meroni, M., et al., *Performance of Spectral Fitting Methods for vegetation fluorescence*
714 *quantification.* Remote Sensing of Environment, 2010. **114**(2): p. 363-374.
715 50. Cogliati, S., et al., *Retrieval of sun-induced fluorescence using advanced spectral fitting methods.*
716 Remote Sensing of Environment, 2015. **169**: p. 344-357.
717 51. Mazzoni, M., et al., *Retrieval of maize canopy fluorescence and reflectance by spectral fitting in the*
718 *O2–A absorption band.* Remote Sensing of Environment, 2012. **124**: p. 72-82.
719 52. Kumar, A.S., et al., *Hyperspectral image clasSIFication by a variable interval spectral average and*
720 *spectral curve matching combined algorithm.* International Journal of Applied Earth
721 Observation and Geoinformation, 2010. **12**(4): p. 261-269.

53. Yves Goulas , A.F., Fabrice Daumard , Sébastien Champagne , and O.M.a.I.M. Abderrahmane Ounis *Gross Primary Production of a Wheat Canopy Relates Stronger to Far Red Than to Red Solar-Induced Chlorophyll Fluorescence.* Remote Sensing, 2017. **9**(97): p. 31.

54. Wood, J.D., et al., *Multiscale analyses of solar-induced florescence and gross primary production.* Geophysical Research Letters, 2017. **44**(1): p. 533-541.

55. Zarco-Tejada, P.J., L. Suarez, and V. Gonzalez-Dugo, *Spatial Resolution Effects on Chlorophyll Fluorescence Retrieval in a Heterogeneous Canopy Using Hyperspectral Imagery and Radiative Transfer Simulation.* IEEE Geoscience and Remote Sensing Letters, 2013. **10**(4): p. 937-941.

56. Yang, X., et al., *Solar-induced chlorophyll fluorescence that correlates with canopy photosynthesis on diurnal and seasonal scales in a temperate deciduous forest.* Geophysical Research Letters, 2015: p. n/a-n/a.

57. Zhang, Q., et al., *Ability of the Photochemical Reflectance Index to Track Light Use Efficiency for a Sub-Tropical Planted Coniferous Forest.* Remote Sensing, 2015. **7**(12): p. 16938-16962.

58. Pradeep Wagle, Y.Z., Cui Jin, and Xiangming Xiao, *Comparison of solar-induced chlorophyll fluorescence, light-use efficiency, and process-based GPP models in maize.* Ecological Society of America~Preprint, 2015.

59. Jenkins, J.P., et al., *Refining light-use efficiency calculations for a deciduous forest canopy using simultaneous tower-based carbon flux and radiometric measurements.* Agricultural and Forest Meteorology, 2007. **143**(1-2): p. 64-79.